Stability of Optical Solitons in Parity–Time-Symmetric Potentials with Competition Nonlinearity

C. Huang*

College of Physics and Materials Science, Tianjin Normal University, 393 Bin Shui West Road, Xi Qing District, Tianjin 300387, China

Received: 09.01.2024 & Accepted: 12.04.2024

Doi: 10.12693/APhysPolA.146.87 *e-mail: chunfuhuang@126.com

This study investigates the existence, stability, and propagation of fundamental, dipole, and tripole modes in parity–time symmetric potentials with competing cubic and quintic nonlinearities. We discuss such parity–time solitons in the presence of a focusing quintic nonlinearity and a defocusing cubic nonlinearity. Assuming a fixed quintic nonlinearity coefficient σ_2 of 1, these solitons can exist and remain stable within a suitable power range. Fundamental solitons can remain stable even for lower values of σ_1, while dipole and tripole solitons may only be stable for larger values of σ_1. By employing appropriate parameters, a significant proportion of solitons can be stabilized. The stability and propagation of the solitons are demonstrated through linear stability analysis and direct numerical simulations.

topics: optical solitons, parity–time (PT) symmetry, stability, cubic and quintic nonlinearity

1. Introduction

Non-Hermitian Hamiltonians with parity–time (PT) symmetry have entirely real eigenvalue spectra, given that the complex potential meets the necessary condition, i.e., $V^*_{PT}(x) = V^*_{PT}(-x)$ [1–5]. The real and imaginary parts of such potentials must display symmetry and antisymmetry with respect to position. Spatial solitons in these PT potentials have been extensively studied in recent years using various nonlinear media, including Kerr media [3–9], saturable nonlinear media [10–12], and non-local media [13–17], among others [18–24]. In addition, spatial solitons have been excited in various PT-symmetric potentials, including the Scarff-II potential, optical lattice potential, harmonic-Gaussian potential, and super-Gaussian potential. Properties such as stability, symmetry breaking, and dynamic evolution have been widely discussed. In recent years, various types of optical solitons have been extensively studied, including bright solitons, gap solitons, dark solitons, vortices, and vector solitons. These solitons are supported by complex PT-symmetric potentials. It is widely accepted that linear PT-symmetric systems have a critical property, namely the existence of a threshold value for the strength of the imaginary component of a complex potential, known as the PT-symmetry breaking point. Once the threshold is surpassed, the spectrum shifts from real-valued to complex-valued. Article [25] provides a comprehensive review of nonlinear waves in PT-symmetric physical systems. In addition to Kerr or cubic nonlinearity, beam propagation has also been studied in media with higher-order nonlinearity. The presence of such nonlinearity significantly modifies beam propagation and can lead to completely new phenomena. Beam stability is achieved with higher-order nonlinearity. The inclusion of the quintic nonlinearity results in the formation of a stable composite soliton, which is not observed in Kerr media. The variational method is used to examine the generation and nonlinear dynamics of multi-dimensional optical dissipative solitonic pulses with the complex cubic–quintic Ginzburg–Landau equation [26]. In physical realizations, the quintic nonlinearity arises from three-body interactions in a dense Bose–Einstein condensate. Observations of cubic–quintic optical nonlinearity have been reported in the crystal, chalcogenide glasses, and ferroelectric films [27–30]. Recent studies have investigated the stability and evolution of solitons in media with competing cubic and quintic nonlinearities [31–37]. This article discusses multipole solitons in PT-symmetric potentials with focusing cubic and de-focusing quintic media [31]. It investigates the fundamental solitons in the cubic–quintic nonlinear Schrödinger equation with PT-symmetric potentials [32]. Additionally, it explores spatial solitons in non-parity–time-symmetric complex potentials with de-focusing

cubic and focusing quintic media [33]. This article analyses stable solitons in the one- and two-dimensional generalized cubic–quintic nonlinear Schrödinger equation with fourth-order diffraction and PT-symmetric potentials [34]. It also studies one-dimensional gap solitons in quintic and cubic–quintic fractional nonlinear Schrödinger equations with a periodically modulated linear potential [35]. Additionally, it presents families of fundamental and multipole solitons in a cubic–quintic nonlinear lattice in fractional dimension [36]. This study examines gap solitons in parity–time-symmetric optical lattices with competing cubic and quintic nonlinearities [37]. The results of [37] indicate that all dipole solitons are unstable, and only a small portion of fundamental solitons are stable when the strength of the focusing quintic nonlinearity is fixed.

After comparing the above-mentioned articles (e.g., [31–37]), we found that most of them have studied the ground state and multipole solitons with focusing cubic and defocusing quintic nonlinearity. However, there are few studies on defocusing cubic and focusing quintic nonlinearity. In particular, there has been relatively little exploration of multipole solitons in PT potentials exhibiting both focusing quintic and defocusing cubic nonlinearity. This study discusses one-dimensional spatial optical solitons in PT single potentials with focusing quintic and defocusing cubic nonlinearity. The model discussed in [31–37], i.e., one-dimensional nonlinear Schrödinger equation, is used to explore multipole solitons in PT single potentials. In this paper, we will consider a complex single potential with real part $V(X) = V_0 \operatorname{sech}^2(X/X_0)$ and imaginary part $W(X) = W_0 \operatorname{sech}(X/X_0) \tanh(X/X_0)$. When V_0, X_0, W_0 are changed, the profile of the real and imaginary components will be modulated. The Schrödinger equation can describe the propagation of a beam in nonlinear media. The nonlinearity in this article is due to cubic and quintic nonlinearities. The competing effects between these two nonlinearities play a significant role in the existence and stability of solitons. The focusing quintic nonlinearity coefficients (σ_2) are fixed at 1, while the coefficients of the cubic nonlinearity (σ_1) are varied from -1 to 0. The results indicate that solitons can exist and be stable within a suitable power range. Fundamental solitons can remain stable even for lower values of σ_1, while dipole and tripole solitons may only be stable for larger values of σ_1. However, it is important to note that these solitons are only stable within a small range of existence when appropriate parameters are employed. The stability of stationary solutions is analysed through linear stability analysis, and their evolution is verified using the beam propagation method.

The paper is organized as follows: In Sect. 2, we present the model and the method used for the linear stability analysis. In Sect. 3, we present a summary of extensive numerical results that outline the stability domains for the fundamental, dipole-, and tripole-bound states. These results are based on the computation of eigenvalues for small perturbations and are corroborated by direct simulations of perturbed propagation dynamics of the solitons. Finally, in Sect. 4, we conclude the results.

2. Theoretical model

This study examines the propagation of one-dimensional spatial optical solitons in PT-symmetric single potentials with competing cubic–quintic nonlinearities. The mathematical model used is the one-dimensional nonlinear Schrödinger equation. Optical waveguides with balanced gain and loss induce linear potentials, which aids in stabilizing various types of self-trapped modes. The propagation of the slowly varying beam envelope $\psi(X,Z)$ can be described by the normalized nonlinear Schrödinger equation, which is also discussed in [31–37],

$$\mathrm{i}\frac{\partial\psi(X,Z)}{\partial Z} + \frac{\partial^2\psi(X,Z)}{\partial X^2} + \sigma_1|\psi|^2\psi(X,Z) + \sigma_2|\psi|^4\psi(X,Z) + V_{PT}\psi(X,Z) = 0, \tag{1}$$

where X and Z are the transverse coordinate and scaled propagation distance, respectively; $\psi(X,Z)$ corresponds to the slowly varying amplitude of the light field; σ_1,σ_2 are the coefficients of the cubic and quintic nonlinearity, respectively; and $V_{PT} = V(X) + \mathrm{i}W(X)$ is the PT-symmetric potential. In the case of PT-symmetry, the potential satisfies the conditions $V(X) = V(-X)$ and $W(-X) = -W(-X)$. Here, the function $V(X)$ describes the real refractive index and $W(X)$ represents the gain-or-loss distribution of the potential.

Now we consider the solution of the form $\psi(X,Z) = \phi(X)\exp(\mathrm{i}\mu Z)$, where μ is a real propagation constant. Then we can obtain the following equation

$$\frac{\partial^2\phi}{\partial X^2} + \sigma_1|\phi|^2\phi + \sigma_2|\phi|^4\phi + V_{PT}\phi = \mu\phi. \tag{2}$$

The modified squared operator method [38] can be used to obtain a localized solution for $\phi(X)$. The stability of this solution was investigated using the Fourier collocation method [39]. The solution of (2) is given by small perturbations $f(X)$, $g(X)$, and is taken to be of the form [31–37]

$$\psi(X,Z) = \phi(X)\exp(\mathrm{i}\mu Z) + \varepsilon\left[f(X,Z)\mathrm{e}^{\lambda Z} + g^*(X,Z)\mathrm{e}^{-\lambda^* Z}\right]\exp(\mathrm{i}\mu Z). \tag{3}$$

Now substituting the expression in (1) and linearising, one gets the following coupled set of linear eigenvalue equations

$$\hat{L}\begin{Bmatrix} f \\ g \end{Bmatrix} = \lambda\begin{Bmatrix} f \\ g \end{Bmatrix}, \tag{4}$$

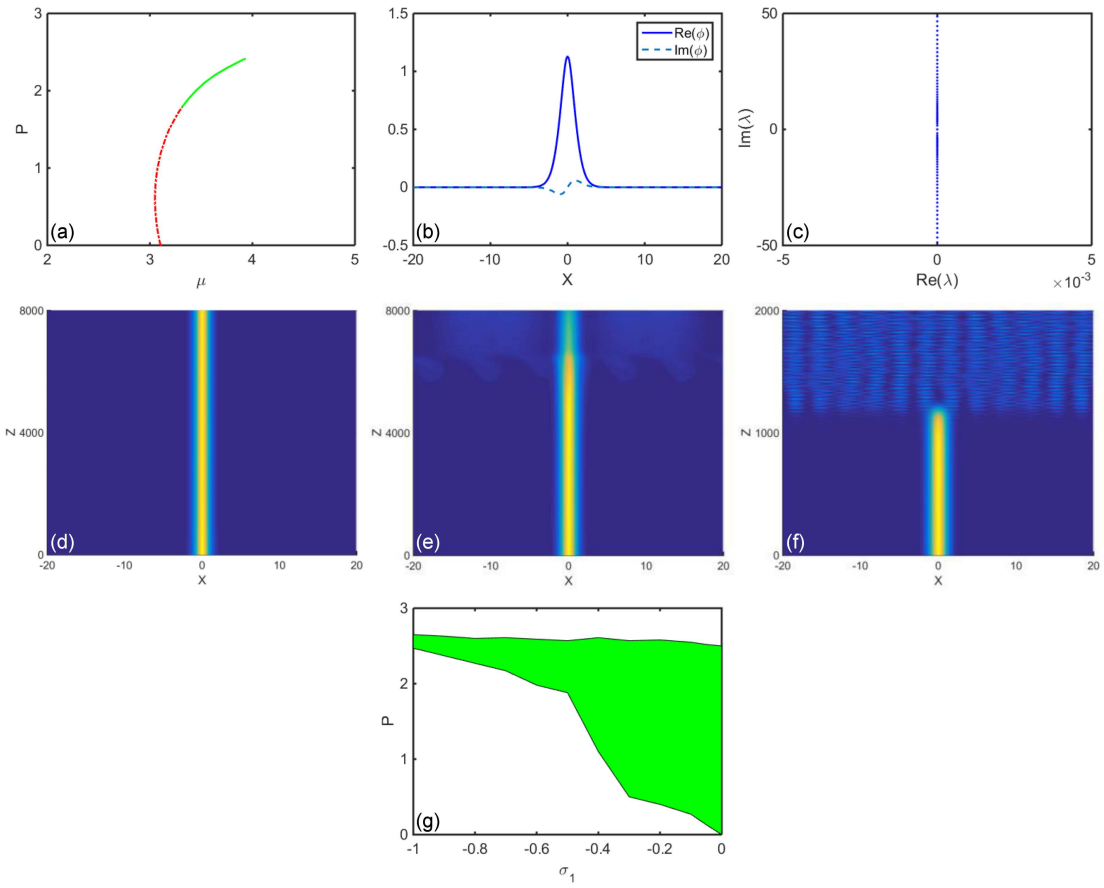

Fig. 1. (a) The dependence of the power P on the propagation constant μ. (b) The solid and dashed curves are, respectively, for real and imaginary parts of fundamental solutions when $P = 2.1$ at $\sigma_1 = -0.5$. (c) Linear stability eigenvalues when $P = 2.1$ at $\sigma_1 = -0.5$. (d, e) Stable or unstable propagations of fundamental modes when $P = 2.1$ and $P = 1.7$ at $\sigma_1 = -0.5$, respectively. (f) Unstable propagation of fundamental soliton for the lower value of σ_1, where $\sigma_1 = -1$, $P = 1.7$. (g) Stable area in green with different values of σ_1. The other parameters are chosen as $V_0 = 4$, $X_0 = 2$, $W_0 = 0.5$.

where

$$\hat{L} = \begin{Bmatrix} \hat{L}_1 & \hat{L}_2 \\ -\hat{L}_2^* & -\hat{L}_1^* \end{Bmatrix}, \tag{5}$$

while $\hat{L}_1 = \partial_{XX} + 2\sigma_1 |\phi|^2 + 3\sigma_2 |\phi|^4 + V_{PT} - \mu$, and $\hat{L}_2 = \sigma_1\phi^2 + 2\sigma_2\phi^3\phi^*$. The symbol "$*$" represents a complex conjugation. The perturbed solution will grow exponentially with Z, resulting in an unstable localized mode if real$(\lambda) \neq 0$. On the other hand, the localized modes are completely stable only when real$(\lambda) = 0$ for every λ (i.e., the system possesses solely imaginary eigenvalues).

3. Stability and evolution of solitons

This discussion concerns the solitons under the focusing quintic nonlinearity and various cubic nonlinearities in the presence of a PT potential. Specifically, let us consider a PT potential with the real part $V(X) = V_0 \mathrm{sech}^2(X/X_0)$ and imaginary part $W(X) = W_0 \mathrm{sech}(X/X_0)\tanh(X/X_0)$. When $X_0 = 1$, the PT potential is the complex Scarf II potential, considered in [1–5]. The profile of the real and imaginary components can be modulated by changing the value of X_0. The same applies to V_0 and W_0. Additionally, the values of σ_1 and σ_2 vary to form these solitons. The stability and propagation properties of the solitons are then described in detail.

Firstly, we will discuss the fundamental solitons. The properties of fundamental solitons are depicted in Fig. 1. The focusing quintic nonlinearity has a fixed coefficient of $\sigma_2 = 1$ throughout this paper, while the coefficient of the cubic nonlinearity σ_1 is varied and ranges from -1 to 0. To maintain generality, let $\sigma_1 = -0.5$, which makes the quintic nonlinearity focusing and the cubic nonlinearity defocusing. The parameters $V_0 = 4$, $X_0 = 2$ and $W_0 = 0.5$ are chosen. The dependence of the propagation constant μ on the power P (i.e., $P = \int_{-\infty}^{\infty} \mathrm{d}x\ |\phi|^2$) is shown in Fig. 1a. This fundamental soliton family exists in the domain where $3.10 \leq \mu \leq 3.92$, while the solitons are stable within the area where $3.32 \leq \mu \leq 3.92$. The stable area is plotted with

a green solid curve. The curve meets either the Vakhitov–Kolokolov (VK) [40, 41] or anti-VK [42] criteria, which serve as necessary conditions for the solitons' stability created by any defocusing or focusing nonlinearity. Solitons exist within a stable range of power, as shown by the curve. This range is bounded by minimum and maximum values, i.e., $P_{\min} \leq P \leq P_{\max}$.

Figure 1b presents the soliton profile, where the solid and dashed curves correspond to the real parts and imaginary sections of fundamental solutions at $P = 2.1$, respectively. It is evident that the solitons with a power of $P = 2.1$ are within the stable area. Figure 1c shows the linear-stability spectrum of this stable soliton where the real parts of all eigenvalues are zero when $P = 2.1$. The numerical study examines the nonlinear evolution of stable and unstable PT solitons under perturbation. Figure 1d, e shows the stable and unstable propagation of soliton mode propagation perturbed with random noise added at a level of 5% of the soliton amplitude at (d) $P = 2.1$ and (e) $P = 1.7$. In the stable case shown in Fig. 1d, the soliton intensity remains unchanged during evolution. In the unstable case depicted in Fig. 1e, the soliton intensity experiences a decrease after stable propagation for a certain distance. It should be noted that the largest real part of the corresponding eigenvalue is very small, with $\max(\mathrm{Re}(\lambda))$ being 0.0011 when $P = 1.7$. Hence, a weak instability corresponding to a very small growth rate is observed.

Specifically, for soliton families to exist under a particular power P, the cubic nonlinearity strength σ_1 must not go beyond a threshold of $\sigma_{\min} \leq \sigma_1 \leq 0$. The fundamental solitons are linearly stable only within a specific portion of their existence region. Numerical simulations indicate that power attains a maximum and a minimum value when σ_1 is between -1 and 0. No fundamental solitons exist when power exceeds the maximum. While if the power is less than the minimum, the fundamental soliton can exist for any value of σ_1 between -1 and 0. For instance, when $P = 2.1$, such fundamental solitons can exist if σ_1 is lower than the threshold, i.e., for $-1 \leq \sigma_1 \leq 0$, these solitons remain stable within the region of $-0.63 \leq \sigma_1 \leq 0$. Numerical calculations indicate that fundamental solitons do not exist when $P > 2.96$, while all fundamental solitons can exist for any value of σ_1 from -1 to 0 when $P < 1.95$. It is important to note that the stability and propagation properties of the solitons are highly sensitive to the values of σ_1. Generally, when σ_1 is increased, $P_{\min}$ decreases more than $P_{\max}$, resulting in an expansion of the stable existence area. Conversely, when σ_1 is decreased, $P_{\min}$ increases more than $P_{\max}$, leading to a shrinkage of the stable existence area. This implies that the stability region is narrower for lower values of σ_1 and wider for larger values of σ_1. Thus, the instability can be increased for lower values of σ_1. Figure 1f illustrates the unstable propagation of the fundamental soliton with $\sigma_1 = -1$ and $P = 1.7$. Evidently, the soliton intensity experiences a sudden decrease after stable propagation for a certain distance. Higher instability leads to shorter distances.

To analyse the stable properties of these solitons, we plotted the stable area for the fundamental solitons with varying values of σ_1. Figure 1g displays the stable area in green. Figure 1g illustrates that fundamental solitons can remain stable even for lower values of σ_1. It is evident that the solitons shown in Fig. 1e, f are not within the stable region. Furthermore, we aim to elucidate the effect of the potential's form on the stability regions of solitons and their impact on the spatial shape of nonlinear modes, as well as the influence of competing nonlinearities. The purpose of this investigation is to examine the role of the PT-symmetric potential on the nonlinear mode characteristics. To achieve this, we perform calculations using different values of the parameters. In general, we observe that the amplitude of the real parts of the fundamental solutions increases with an increase in V_0, however, it decreases with an increase in W_0 and X_0 at a particular power. Conversely, the amplitude of the imaginary part exhibits the opposite behaviour. In general, the stability regions of solitons will be enlarged for higher values of V_0 and lower values of W_0. Most importantly, the power P of the stable soliton decreases with the decrease in X_0, and the stable region of solitons expands. For instance, when $X_0 = 1.5$, the solitons are stable within the area where $0.55 \leq P \leq 2.15$, given the parameters $V_0 = 4$, $W_0 = 0.5$, $\sigma_1 = -0.5$. There are additional stable solitons for various values of σ_1 ranging from -1 to 0, and the stable region has expanded. Under the same conditions, the solitons are more stable for lower values of X_0.

Next, we will explore the dipole instances, as depicted in Fig. 2, which illustrates typical images of dipole solitons. For the value of σ_1, we chose -0.2, while other parameters were selected as follows $V_0 = 4$, $X_0 = 2$, $W_0 = 0.5$. The power curve of the dipole solitons is presented in Fig. 2a, revealing a clear pattern of increase in power of the dipole solitons with the propagation constant μ. Dipole soliton exists in the domain where $0 \leq P \leq 4.70$, and the solitons are stable within the area where $0.50 \leq P \leq 1.54$. The dipole soliton exists within a specific domain, and it stabilizes within a defined zone, as demonstrated by the solid green curve. The solid and dashed curves in Fig. 2b display, respectively, the real and imaginary components of dipole solutions at power level $P = 1$. Additionally, Fig. 2c exhibits the linear stability spectrum of the stable soliton where the real portions of all eigenvalues are zero. It is evident that the dipole solitons with power $P = 1$ exist within the stable region. Furthermore, we have conducted a numerical analysis of the nonlinear evolution of both stable and unstable dipole solitons under perturbation. In Fig. 2d and Fig. 2e, the stable and unstable propagations of dipole solitons are shown

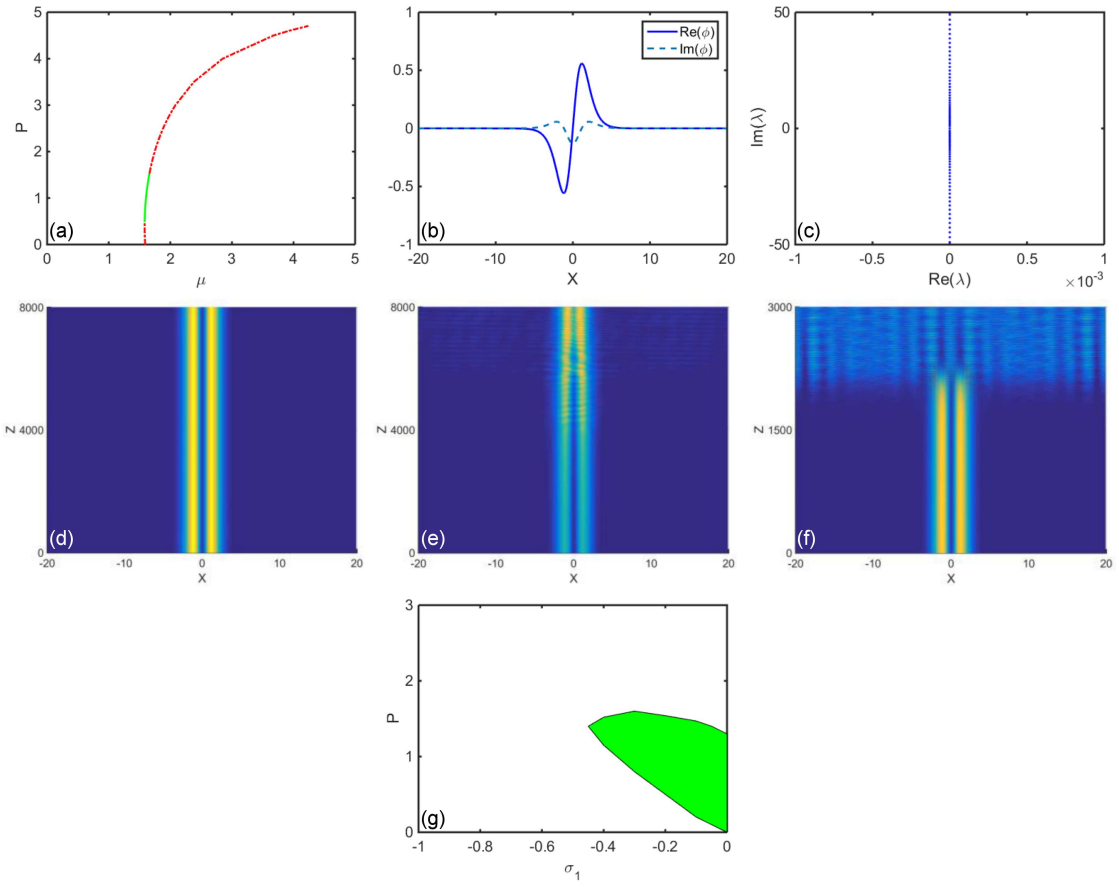

Fig. 2. (a) The dependence of the propagation constant μ on the power P. (b) The solid and dashed curves are for real and imaginary parts of dipole solutions when, respectively, $P = 1$ at $\sigma_1 = -0.2$. (c) Linear stability eigenvalues when $P = 1$ at $\sigma_1 = -0.2$. (d, e) Stable or unstable propagations of nonlinear dipole modes when $P = 1$ and $P = 1.8$ at $\sigma_1 = -0.2$, respectively. (f) Unstable propagation of dipole soliton when $P = 1$ at $\sigma_1 = -0.5$. (g) Stable area in green with different values of σ_1. The parameters are chosen as $V_0 = 4$, $X_0 = 2$, $W_0 = 0.5$.

at $P = 1$ and $P = 1.8$, respectively. Figure 2d demonstrates the robustness of dipole solitons as their intensity remains unchanged during evolution. However, in the unstable case shown in Fig. 2e, the soliton intensity decreases after stable propagation over a certain distance. The maximum real part of the corresponding eigenvalue is extremely small, with $\max(\mathrm{Re}(\lambda))$ being 0.0025 at $P = 1.8$. Such a weak instability is indicative of a very small growth rate. The effect of competing cubic and quintic nonlinearities varies depending on the value of σ_1. In general, it is easy to generate dipole solitons for any value of σ_1 ranging from -1 to 0 for a specific power P. However, the stable region is narrow in a specific section of their existence area. For instance, when given $P = 1$, in order for these dipole solitons to exist and remain stable, σ_1 should be within the range of $-0.35 \leq \sigma_1 \leq 0$. Dipole solitons become unstable when $\sigma_1 < -0.35$. We vary σ_1 over the range of -1 to 0, observing the typical unstable propagation of the dipole soliton for lower values of σ_1. Figure 2f illustrates this phenomenon with $\sigma_1 = -0.5$ and $P = 1$. It is evident that the soliton intensity undergoes changes during its propagation. In general, dipole solitons tend to be unstable for lower values of σ_1 but are relatively stable for larger values. This can be observed by comparing Fig. 2d and Fig. 2f.

In summary, Fig. 2g displays the stable area in green for these dipole solitons with varying values of σ_1. Figure 2g shows that dipole solitons may only be stable for larger values of σ_1. It is clear that the dipole solitons in Fig. 2e, f are not within the stable area. In this study, we investigate the impact of competing nonlinearities on the stability of solitons, as well as the influence of the PT-symmetric potential on the nonlinear mode characteristics. The amplitude of the real parts of the dipole soliton solutions generally increases with an increase in V_0 but decreases with an increase in W_0 and X_0 at a particular power. Conversely, the amplitude of the imaginary part exhibits the opposite behaviour. In general, the power decreases as X_0 decreases under the same conditions. The stability regions of solitons will be enlarged for higher values of V_0 and lower values of W_0, while they will shrink with the

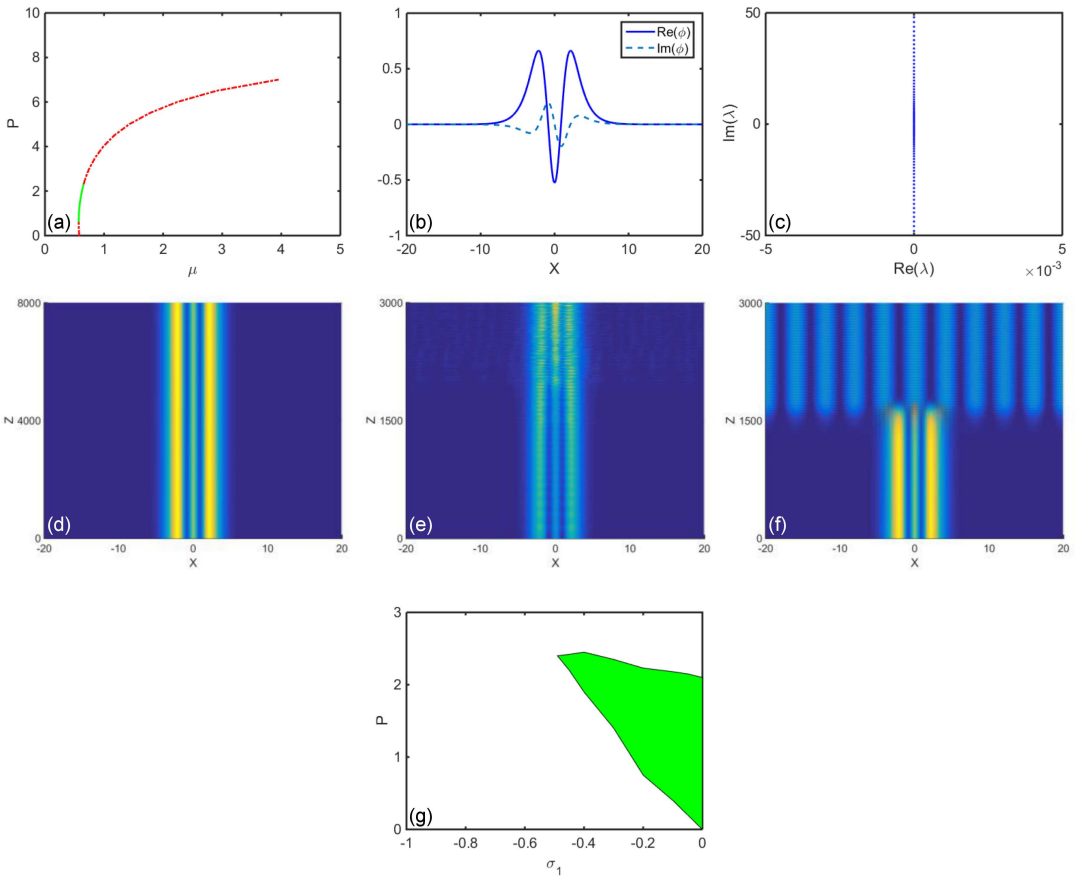

Fig. 3. (a) The dependence of the power P on the propagation constant μ. (b) The solid and dashed curves are for, respectively, the real and imaginary parts of tripole solutions when $P = 2$ at $\sigma_1 = -0.2$. (c) Linear stability eigenvalues when $P = 2$ at $\sigma_1 = -0.2$. (d, e) Stable or unstable propagations of nonlinear tripole modes when, respectively, $P = 2$ and $P = 2.6$ at $\sigma_1 = -0.2$. (f) Unstable propagation of tripole soliton when $P = 2$ at $\sigma_1 = -0.5$. (g) Stable area in green with different values of σ_1. The parameters are chosen as $V_0 = 4$, $X_0 = 2$, $W_0 = 0.5$.

decrease in X_0. For example, when $X_0 = 1$, there are no stable dipole solitons when $\sigma_1 \leq -0.38$, given the parameters $V_0 = 4$ and $W_0 = 0.5$. Generally, the stability region is narrower for lower values of σ_1 and wider for larger values of σ_1. Thus, the instability can be increased for lower values of σ_1. It should be noted that all solitons are affected by random noise, which is added at a level of 5% of the soliton amplitude at the input.

Finally, we will now consider the tripole cases. Figure 3 displays typical images of tripole solitons. Here, σ_1 is set to -0.2, while the other parameters are as follows: $V_0 = 4$, $X_0 = 2$, $W_0 = 0.5$. In Fig. 3a, we can observe the power curve of the tripole solitons. The tripole soliton family exists within the domain $0 \leq P \leq 7.0$, while the solitons are stable within the area $0.78 \leq P \leq 2.23$. The stable area is displayed as a green solid curve. Figure 3b shows the real (solid curves) and imaginary (dashed curves) parts of tripole solutions when $P = 2$. Figure 3c shows the linear-stability spectrum of the stable soliton, where the real parts of all eigenvalues are zero when $P = 2$. The stable region consists of tripole solitons with power $P = 2$. To confirm the findings of the linear stability analysis, we numerically simulated equation (1) to propagate the stationary solution. We perturbed tripole solitons with a 5% random noise and summarized the subsequent soliton evolutions in Fig. 3d, e. The results show that the intensity of the stable soliton mode propagation remains constant, while in the unstable case, it decreases. The power value of $P = 2$ in Fig. 3d falls within the stable region. However, the power value of $P = 2.6$ in Fig. 3e does not fall within the stable region. In the unstable case, the maximum real part of the corresponding eigenvalue is very small, with a maximum of $\mathrm{Re}(\lambda) = 0.0034$ when $P = 2.6$. Therefore, the growth rate is low for weak instability. When considering a particular power P, it is possible to form tripole solitons for any value of σ_1 from -1 to 0. However, their existence is limited to a narrow stable region. The competition between cubic and quintic nonlinearities changes as σ_1 varies from -1 to 0. For example, tripole solitons remain stable when $P = 2$ and σ_1 varies between -0.41 and 0, but they become

unstable when σ_1 decreases. Figure 3f displays the typical unstable propagation of a tripole soliton for a lower value of σ_1, where $\sigma_1 = -0.5$, $P = 2$. Upon comparison with Fig. 3d, f, it becomes clear that the tripole soliton can indeed be stable for a larger value of σ_1. However, for a lower value of σ_1, it becomes difficult for the tripole soliton to remain stable.

To summarise, Fig. 3g displays the stable area in green for tripole solitons with varying values of σ_1. Figure 3g shows that tripole solitons may only be stable for larger values of σ_1. It is evident that the tripole solitons illustrated in Fig. 3e, f are outside the stable region. In this study, we also investigate the impact of the PT-symmetric potential on the nonlinear mode characteristics and stability properties. Our findings indicate that, in general, the amplitude of the real parts of the tripole soliton solutions increases with an increase in V_0 but decreases with an increase in W_0 and X_0 at a particular power. Conversely, the amplitude of the imaginary part exhibits the opposite behaviour. Under the same conditions, the stability regions of solitons will be enlarged for higher values of V_0 and lower values of W_0. It is difficult to form stable solitons for very low values of X_0. Generally, the power of stable solitons decreases as X_0 increases. Tripole solitons exist when the power exceeds the minimum and is less than the maximum at a certain σ_1. The stability region is narrower for lower values of σ_1 and wider for larger values of σ_1.

Furthermore, we conducted numerous numerical simulations with alternative parameters, which yielded comparable findings. Solitons are able to exist, remain stable within a suitable power range, and sustain stability for a larger value of σ_1. A considerable proportion of solitons can be stabilized by employing appropriate parameters.

4. Conclusions

In conclusion, this study examines the existence, stability, and propagation of fundamental, dipole, and tripole modes in PT potentials with competing cubic and quintic nonlinearity. The case of PT solitons under focusing quintic nonlinearity and various defocusing cubic nonlinearity is discussed. The competing effect between cubic and quintic nonlinearities plays a significant role in the existence and stability of both fundamental and multi-pole PT solitons. The focusing quintic nonlinearity coefficients (σ_2) are fixed at 1, while the coefficients of the cubic nonlinearity (σ_1) are varied from -1 to 0. The results indicate that solitons can exist and be stable within a suitable power range, with greater stability observed for larger values of σ_1. Fundamental solitons can remain stable even for lower values of σ_1, while dipole and tripole solitons may only be stable for larger values of σ_1. These solitons may be stable within a small range of existence by employing appropriate parameters. Linear stability analysis was conducted to investigate the stability of these stationary solutions. Additionally, direct numerical simulations were used to explore the propagation of these solutions.

References

[1] C.M. Bender, S. Boettcher, *Phys. Rev. Lett.* **80**, 5243 (1998).

[2] C.M. Bender, *Rep. Prog. Phys.* **70**, 947 (2007).

[3] Z.H. Musslimani, K.G. Makris, R. El-Ganainy, D.N. Christodoulides, *Phys. Rev. Lett.* **100**, 030402 (2008).

[4] K.G. Makris, R. El-Ganainy, D.N. Christodoulides, Z.H. Musslimani, *Phys. Rev. Lett.* **100**, 103904 (2008).

[5] Z.H. Musslimani, K.G. Makris, R. El-Ganainy, D.N. Christodoulides, *J. Phys. A Math. Theor.* **41**, 244019 (2008).

[6] C. Huang, J. Zeng, *Opt. Laser Technol.* **88**, 104 (2017).

[7] X. Li, L. Wang, Z. Zhou, Y. Chen, Z. Yan, *Nonlinear Dyn.* **108**, 4045 (2022).

[8] N. Ghosh, A. Das, D. Nath, *Nonlinear Dyn.* **111**, 1589 (2023).

[9] L. Dong, L. Gu, D. Guo, *Phys. Rev. A* **91**, 053827 (2015).

[10] P. Li, C. Dai, R. Li, Y. Gao, *Opt. Exp.* **26**, 6949 (2018).

[11] T.D. Haji, T.M. Solaimani, M. Ghalandari, B. Babayar-Razlighi, *Phys. Scr.* **96**, 125531 (2021).

[12] X. Zhu, W. Che, Z. Wu, J. Xie, Y. He, *J. Opt.* **22**, 035503 (2020).

[13] X. Zhu, X. Peng, Y. Qiu, H. Wang, Y. He, *New. J. Phys.* **22**, 033035 (2020).

[14] Z. Shi, H. Li, X. Zhu, X. Jiang, *Europhys. Lett.* **98**, 64006 (2012).

[15] J. Huang, Y. Weng, H. Wang, *Opt. Exp.* **26**, 11667 (2018).

[16] J. Yang, *Phys. Rev. E* **98**, 042202 (2018).

[17] P.J. Chen, H. Wang, *Opt. Exp.* **31**, 30529 (2023).

[18] L. Qin, C. Hang, Z.Y. Shi et al., *Opt. Exp.* **31**, 11116 (2023).

[19] S. Bhatia, A. Goyal, S. Jana, C.N. Kumar, *Phys. Lett. A* **469**, 128751 (2023).

[20] W.B. Bo, R.R. Wang, W. Liu, Y.Y. Wang, *Chaos* **32**, 093104 (2022).

[21] M. Bagci, *Phys. Rev. A* **103**, 023530 (2021).

[22] E. Luz, V. Lutsky, E. Granot, B.A. Malomed, *Sci. Rep.* **9**, 4483 (2019).

[23] M. Ögren, F.K. Abdullaev, V.V. Konotop, *Opt. Lett.* **42**, 4079 (2017).

[24] Y. Zhong, H. Triki, Q. Zhou, *Nonlinear Dyn.* **112**, 1349 (2024).

[25] B.A. Malomed, D. Mihalache, *Rom. J. Phys.* **64**, 106 (2019).

[26] V. Skarka, N.B. Aleksic, *Acta Phys. Pol. A* **112**, 791 (2007).

[27] C. Zhan, D. Zhang, D. Zhu et al., *J. Opt. Soc. Am. B* **19**, 369 (2002).

[28] E.L. Falcao-Filho, C.B. de Araujo, J.J. Rodrigues Jr., *J. Opt. Soc. Am. B* **24**, 2948 (2007).

[29] K. Ogusu, J. Yamasaki, S. Maeda, M. Kitao, M. Minakata, *Opt. Lett.* **29**, 265 (2004).

[30] B. Gu, Y. Wang, W. Ji, J. Wang, *Appl. Phys. Lett.* **95**, 041114 (2009).

[31] P. Li, L. Li, D. Mihalache, *Rom. Rep. Phys.* **70**, 408 (2018).

[32] G. İzzet, A. Nalan, B. İlkay, *Opt. Commun.* **354**, 277 (2015).

[33] X. Zhu, Z. Cai, J. Liu, S. Liao, Y. He, *Nonlinear Dyn.* **108**, 2563 (2022).

[34] N.T. Nkouessi, G.C. Tiofack Latchio, A. Mohamadou, *Eur. Phys. J. D* **74**, 32 (2020).

[35] L. Zeng, J. Zeng, *Nonlinear Dyn.* **98**, 985 (2019).

[36] L. Zeng, D. Mihalache, B.A. Malomed, X. Lu, Y. Cai, Q. Zhu, J. Li, *Chaos Solitons Fract.* **144**, 110589 (2021).

[37] L. Ge, M. Shen, T. Zang, C. Ma, L. Dai, *Phys. Rev. E* **91**, 023203 (2015).

[38] J. Yang, T.I. Lakoba, *Stud. Appl. Math.* **118**, 153 (2007).

[39] J. Yang, *J. Comput. Phys.* **227**, 6862 (2008).

[40] N. Vakhitov, A. Kolokolov, *Radiophys. Quantum Electron.* **16**, 783 (1973).

[41] L. Berge, *Phys. Rep.* **303**, 259 (1998).

[42] H. Sakaguchi, B.A. Malomed, *Phys. Rev. A* **81**, 013624 (2010).